Towards an Underwater 3D Laser Scanning System for Mobile Mapping

Michael Bleier[1], Joschka van der Lucht[1], and Andreas Nüchter[1]

***Abstract*—Digitizing archaeological or industrial sites on land using standard methods of photogrammetry like 3D modeling from photos or laser scanning is well understood. In contrast, precise underwater surveying with high resolution is still a complex and difficult task. In this paper, we present the development and construction of a structured light underwater laser scanning system and show first results on applying the system for mobile scanning in the water. The laser scanner employs two line lasers to project a cross on the scene. This enables mobile scanning in multiple directions and provides an overlapping scan pattern, which is exploited for trajectory optimization. We describe the image processing, calibration and 3D reconstruction methods used for creating point clouds using the system. In experiments conducted in a towing tank we demonstrate 3D scans captured by rotating the scanner on a robotic joint and first results of mobile scans acquired by moving the scanner through the water along a linear trajectory.**

I. Introduction

Cultural Heritage sites and archaeological ruins are the legacy of civilization and evolution but they are severely threatened by natural deterioration and man-made alteration and robbery. Many sites are in need for precise digitization for the preservation of sensitive assets and their dissemination to the general public. Unfortunately, the constraints and requirements for each specific site vary and, therefore, not a single sensor system fits all sites and purposes. While digitizing archaeological sites on land as well as artifacts are well understood and standard methods of photogrammetry like 3D modeling from photos or laser scanning are applied, precise underwater surveying with high resolution is still a complex and difficult task.

For many underwater mapping applications sonar technology is still the primary solution because of its large sensor range and its robustness to turbidity. However, certain measurement tasks require higher accuracies and resolutions. For example, archaeologists are interested in scanning and monitoring wooden structures, such as fragments of hull planks of ships, with millimeter resolution and accuracy to be able to investigate which parts fit together. Recovering these artifacts from the water and scanning them on land might lead to wrong conclusions because drying the wood causes deformations. Furthermore, there is also an interest in high resolution underwater scanning for industrial applications, such as inspection of welding seams, surveying of pipelines and structural monitoring of the pillars of oil platforms or offshore wind farms. Such requirements make optical scanners interesting despite their limited range due to the high absorption of light in water. In the field of archaeology photogrammetric methods are regularly applied to underwater sites [1].

[1]The authors are with Informatics VII: Robotics and Telematics, Julius-Maximilians-University, Am Hubland, Würzburg 97074, Germany. {michael.bleier, joschka.lucht, andreas.nuechter}@uni-wuerzburg.de

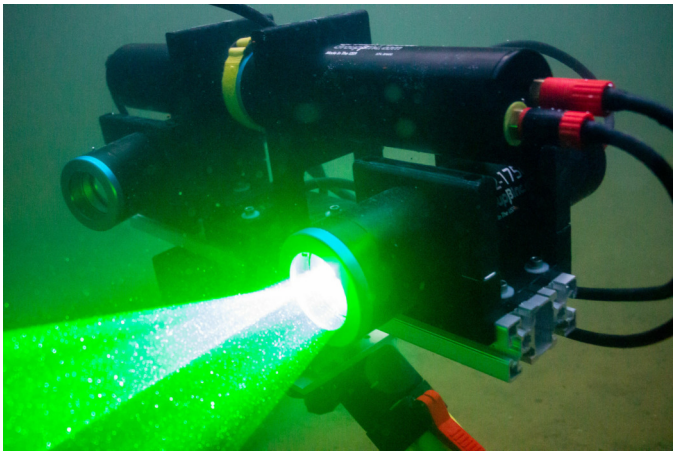

Fig. 1. Developed structured light underwater scanning system with cross laser line projector deployed for testing in a natural lake.

In this paper, we present work in progress on the development and construction of a structured light underwater laser scanning system for mobile mapping applications. Figure 1 depicts the scanner mounted on a tripod and deployed for testing in a natural lake. The system is built using off-the-shelf underwater housings, aluminum profiles and 3D printed parts. We use high power green line lasers to project a cross pattern on the scene. This has the advantage that for mobile mapping applications the scanner can be moved into multiple directions, while still a large swath is scanned. Using two line projectors has the advantage that there is overlap between the point clouds created from the individual lines even if the scanner is moved along a linear trajectory. These measurements of the same surface at different points in time are exploitable for trajectory optimization using Simultaneous Localization and Mapping (SLAM) algorithms.

II. Related Work

A comprehensive overview of optical underwater sensing modalities is given in [2]. Different variants of structured light scanning have been successfully applied for underwater 3D scanning. Fringe projection has been applied successfully to acquire very detailed scans with high precision of small underwater objects [3], [4]. Despite the limited illuminating

power of a standard digital projectors, working distances of more than $1\,\mathrm{m}$ have been reported in clear water [5].

Underwater laser scanning systems with larger measurement range often employ high-power line laser projectors. For example, commercial scanners from 2G Robotics offer a range of up to 10 m depending on the water conditions [6]. 3D scans are typically created by rotating the scanner and measuring the movement using rotational encoders or mounting the scanner to a moving platform.

Palomer et al. use a laser projector based on galvanometer scanners [7]. This allows to project sweeping laser lines on the scene, which allows to reconstruct the full field of view of the camera. Since in this configuration the laser hits the air-glass and glass-water interface surface at an angle, in water the laser projection cannot be described by a plane. This needs to be modeled explicitly using a physical refraction model. For example, Palomer et al. calibrate the parameters of a cone model to describe the laser projection surface [8].

Another approach is to mount line laser projectors inside a glass cylinder and rotate the line lasers with a motor. This approach is, for example, used in the UX-1 underwater mine exploration robotic system [9]. In this case the line projectors are aligned manually, such that the projection is perpendicular to the air-glass and glass-water interface surfaces and a straight line is projected. This way the refraction effects are relatively small and are neglected depending on the accuracy requirements. Similarly, the SeaVision subsea 3D laser imaging system developed by Kraken Robotics [10] uses rotating red, green and blue line lasers. This enables the system to produced colored scans by evaluating the intensity of the responses of the different laser projectors. Alternatively, diffractive optical elements are used to project multiple lines or a grid for one shot 3D reconstruction [11], [12]. Calibration of these systems is typically achieved using chessboard patterns or 3D calibration fixtures. Some of the parameters can also be determined using self-calibration approaches [13].

Most of the commercially available underwater laser range sensors are based on laser stripe projection or other forms of structured light. More recently companies started development of time-of-flight (ToF) underwater laser scanners. For example, the company "3D at Depth" developed a commercial underwater LiDAR, which is mounted on a pan-and-tilt unit to create 3D scans of underwater environments similar to terrestrial pulsed ToF laser scanning [14]. A recently proposed scanning system by Mitsubishi uses a dome port with the scanner aligned in the optical center to achieve a wider field of view [15].

Mobile mapping with underwater laser scanners is achieved by using the navigation data of the vehicle. For example, Global Navigation Satellite System (GNSS) data of a ship [16] or a combination of acoustic underwater positioning system information, Doppler Velocitiy Log (DVL) and inertial navigation [9] is used to measure the vehicle trajectory. Furthermore, Structure-from-Motion (SfM) algorithms are applied to create a trajectory estimate of the scanning system [17].

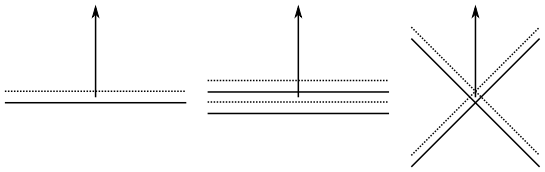

Fig. 2. Overlap of scan patterns for different laser line configurations. Left: single line, middle: two parallel lines, right: cross line. The arrow visualizes the direction of movement.

III. Structured Light Underwater Laser Scanner

The data presented in this paper was captured with a self-built structured light underwater laser scanning system. We choose high power laser line projectors because of the high absorption of light especially in turbid water conditions. Moreover, when scanning in surface water ambient light from the sun is an issue. The laser projection needs to be bright enough, such that sufficient contrast from ambient illumination is achieved. High power lasers and high sensitivity cameras with large dynamic range mitigate these problems to some degree.

Fig. 2 shows different scan patterns: single laser line, two parallel lines and cross line configuration. Compared to a single laser line configuration scanning using multiple laser lines has the advantage that internal overlap between the created point clouds of the individual line projection is achieved. With a single line we usually only have overlap between the point clouds of individual laps of the vehicle that is carrying the scanner. Additionally, with a cross line configuration a large swath can be also scanned for across-track movement. This means scanning along a trajectory which is perpendicular to the direction of movement visualized by the arrow in Fig. 2. Therefore, we choose a cross line laser pattern because this enables scanning with mostly unrestricted movement. Only the distance between the scanner and the object has to be kept in a certain range, because of field-of-view and focus restrictions.

The two laser planes are projected at an angle of $45\,\mathrm{deg}$ with respect to the vertical camera axis. This way both projected laser lines have approximately the same baseline. However, the resulting baseline is reduced compared to the mounting distance of the camera and laser projector housings.

A. Underwater Scanner Hardware

The developed structured light underwater laser scanner consists of two housings with flat port glass windows, one containing the camera and the other one the cross line laser projector. The system is depicted in the left image in Figure 3. The two housings are mounted on a $0.5\,\mathrm{m}$ long aluminum bar. Custom mounts for the housings were manufactured using 3D-printing. The camera housing is mounted at an angle of $30°$ to the bar. On top, a larger housing with lithium polymer batteries is mounted, which allows up to 6 hours of scanning time. This housing also contains the motor control electronics and a network switch to connect the underwater scanner to the surface via an underwater cable. The scanner is placed on a robotic joint with slewing ring bearings and a 1:50

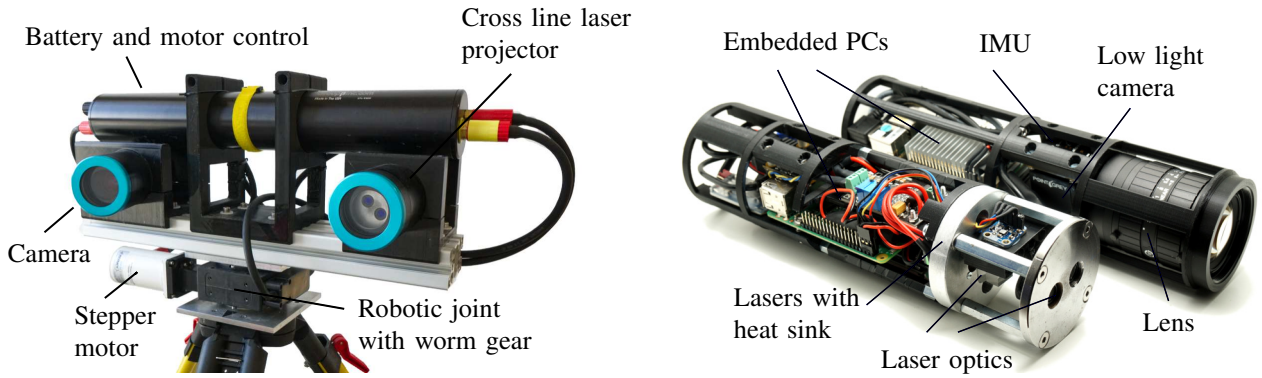

Fig. 3. Structured light underwater laser scanner. Left: Scanner with motorized robotic joint mounted on a tripod, right: Detail view of the camera and laser projector assemblies mounted inside the underwater housings.

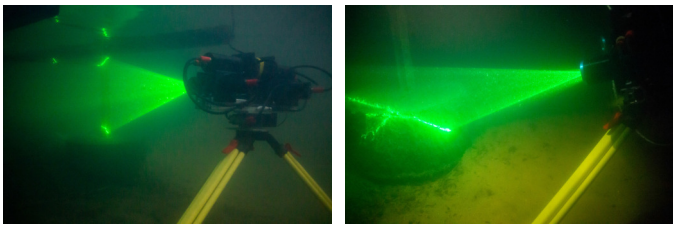

Fig. 4. Developed structured light underwater laser scanning system deployed for testing in a natural lake. Left: 3D underwater scanner with cross line laser projection, right: 3D-scanning of the concrete base of a footbridge.

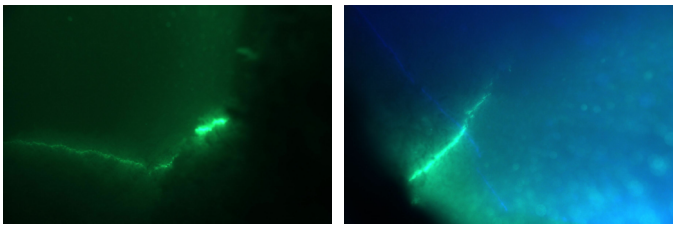

Fig. 5. Example images captured with green and blue laser projectors in turbid water conditions with less than $1\,\mathrm{m}$ visibility.

worm gear, which is driven by a stepper motor. This allows rotating the scanner to capture $360\,\mathrm{deg}$ scans. A magnetic encoder sealed in epoxide resin is used to measure the rotation angle of the scanner. All housings include embedded PCs with network interface. The Robot Operating System (ROS) is used as a middleware for sensor interfaces, logging and data processing. All embedded PCs are time-synchronized using Network Time Protocol (NTP) and a pulse-per-second signal. For synchronization of the camera with the laser projector a dedicated trigger pulse signal is used.

The right image in Figure 3 shows the electronics and optics components mounted inside the underwater housings. The camera assembly includes the lens with a focal length of $12.5\,\mathrm{mm}$. The camera is a FLIR Blackfly 2.3 Megapixel color camera with a $1/1.2$" Sony Pregius IMX249 CMOS sensor. The image resolution is 1920×1200 pixels with $5.86\,\mu\mathrm{m}$ pixel size and a maximum framerate of $41\,\mathrm{fps}$. For image processing an embedded PC with an Intel Atom x5-Z8350 processor is included in the housing.

The cross line projector is constructed from Powell laser line optics, beam correction prisms and the laser diodes. The lasers are two $1\,\mathrm{W}$ green diode lasers with a wavelength of $525\,\mathrm{nm}$, which are mounted to an aluminum heat sink. The laser output power is controlled by two laser diode drivers, which can be adjusted via PWM signals generated by a microcontroller connected to an embedded PC. The two laser lines project a laser cross consisting of two perpendicular lines in the scene. The fan angle of the laser lines is $45\,\mathrm{deg}$, which is reduced in water to approximately $32\,\mathrm{deg}$. The total field of view is therefore $360\,\mathrm{deg} \times 32\,\mathrm{deg}$. The lasers are fired synchronized to the camera shutter using trigger pulse signals. An alternating firing order of the individual lasers is employed, such that each image captured by the camera includes only one of the two laser lines.

Figure 4 depicts the scanner mounted on a tripod and deployed for testing in a natural lake. All components of the scanner are rated for $100\,\mathrm{m}$ water depth. The main components of the scanner, such as the underwater housings, cables and connectors are rated for more than $1000\,\mathrm{m}$ water depth.

B. Image Processing

Significant challenges for underwater 3D laser scanning lie in the image processing and extraction of the laser curves. Figure 5 shows images captured using the underwater system in turbid water conditions. Particle backscatter complicates the automatic extraction of the laser lines. This requires research into improved image processing algorithms for robust extraction of the laser curves.

For the extraction of the laser lines in the image, we employ a ridge detector based on the work of Steger [18]. The idea of the algorithm is to find curves in the image that have a characteristic 1D line profile in the direction perpendicular to the line, i.e., a vanishing gradient and high curvature. We apply the line detector to a gray image created by averaging the color channels.

Since the line detector requires applying computational expensive convolution filters, we first segment the image based

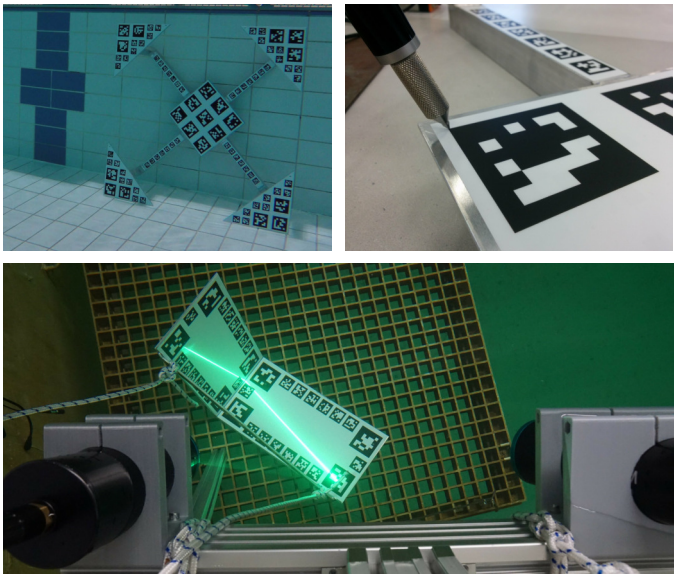

Fig. 6. 3D calibration fixtures. Top: Structure for camera calibration and measurement of tag positions using the iSpace position and tracking system, bottom: L-shaped calibration target for estimating the laser plane parameters.

on color cues and intensity thresholds. This way the line extraction algorithm needs to be computed only for parts of the image, which significantly reduces processing time.

C. Calibration

We calibrate the underwater laser scanner in air and water using the same method. We calibrate the camera using Zhang's method [19] with a 3D calibration fixture featuring AprilTags [20] as fiducial markers. The advantage over chessboard of circle patterns is that calibration points are extracted automatically even if only part of the structure is visible in the image. The employed structure is depicted in the top images of Figure 6. It is constructed from aluminum sheets and profiles using welding. The pattern is printed on vinyl waterproof stickers and glued on the structure. The position of the individual tags are measured using the iSpace high-precision position and tracking system from Nikon Metrology, which provides sub-millimeter accuracy [21].

For calibrating the laser projector it is necessary to determine the laser plane parameters relative to the origin of the camera coordinate system. To do this, an L-shaped 3D calibration pattern, depicted in the bottom image of Figure 6, consisting of two planes with AprilTags has been designed. This enables determining the laser plane equation from a single image.

First, we detect the L-shaped pattern in the camera image and compute the pose relative to the calibrated camera. From this we compute the parameters of the two individual planes of the calibration target. Then, we detect laser points lying on the two calibration planes and reconstruct their 3D position by intersecting the camera ray with the respective calibration plane. The plane parameters of the laser plane is finally found by fitting a plane to the reconstructed 3D laser point positions.

To obtain robust parameter estimates we capture images with different calibration fixture poses. Then, we compute the best fitting plane over multiple calibration images to improve the final solution.

The rotation axis is estimated by placing the 3D calibration fixture in front of the scanner and rotating the system. The relative movement of the camera is estimated by computing the pose relative to the calibration pattern using the intrinsic camera parameters. The rotation is measured using the rotary encoder feedback. Then, the translation and rotation offsets of the camera coordinate system with respect to the rotation center of the motor are found by optimization. The offset parameters are computed by minimizing the difference between the relative pose measurements based on the calibration fixture and the rotary encoder.

IV. Experimental Results

For testing and evaluation the underwater laser scanner was deployed in the towing tank at the chair of fluid dynamics at the University of Rostock. The towing carriage and tank is depicted in the left image of Figure 7. The water tank is $5\,\mathrm{m}$ wide and provides a depth of up to $3\,\mathrm{m}$. The scanner was deployed at about $2.5\,\mathrm{m}$ water depth using a vertical bar, which is shown in the middle image of Figure 7.

A. Underwater 3D Scanning Results

Static scans were acquired by rotating the system using the yaw motor of the scanner. For evaluation purposes complex objects built by the Fraunhofer Research Institution for Large Structures in Production Engineering (IGP) in Rostock and the company IMAWIS GmbH are placed in front of the scanner at different distances. The test objects shown in the right image of Figure 7 are scanned in air with a high precision structured light scanner GOM ATOS III to create a reference model of the geometry [22].

Figure 8 shows in the left column point cloud results captured at varying distances. The point clouds are colored by intensity. The top scan was captured at about $1\,\mathrm{m}$ distance, the middle scan at $2\,\mathrm{m}$ distance, and the bottom scan at $3.5\,\mathrm{m}$ distance from the objects. The point clouds are registerd using the Iterative Closest Point (ICP) algorithm with the reference models. This is depicted in the images in the middle column of Figure 8.

We compute the distance between the reference model and the captured point cloud. The scan colored by the difference to the reference model is visualized in the right column of Figure 8. Note that the color scaling is adjusted for each picture to the range of errors present in the particular scan to highlight the distribution of errors within the scan. While for the close range small errors in the range of millimeters is observed, the error significantly increases with distance. For the top scan captured at $1\,\mathrm{m}$ distance the errors are below $1\,\mathrm{cm}$. The middle scan captured at $2\,\mathrm{m}$ shows larger errors of up to $2\,\mathrm{cm}$. The bottom scan captured at $3.5\,\mathrm{m}$ distance shows errors of up to $5\,\mathrm{cm}$. At the larger scanning distances some

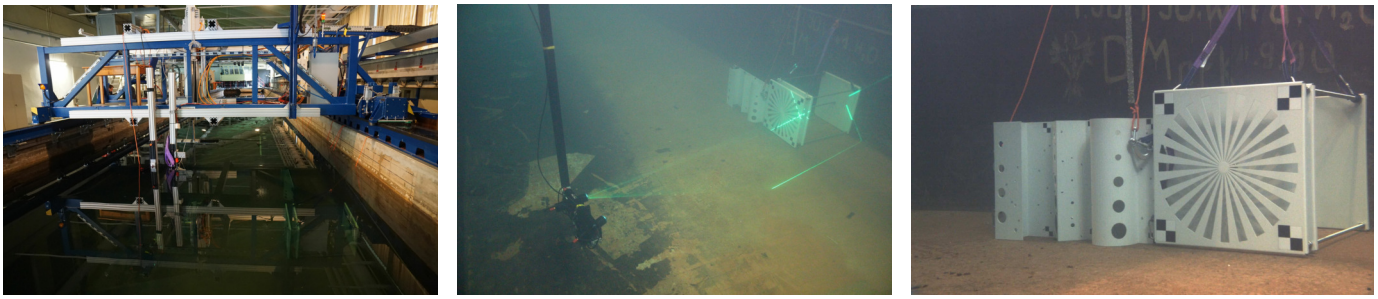

Fig. 7. Mobile mapping experiments conducted in the towing tank of the chair of fluid dynamics at the University of Rostock. Left: towing tank at the chair of fluid dynamics in Rostock, middle: structured light scanner deployed in the tank, right: image of the test objects captured with the camera of the scanner.

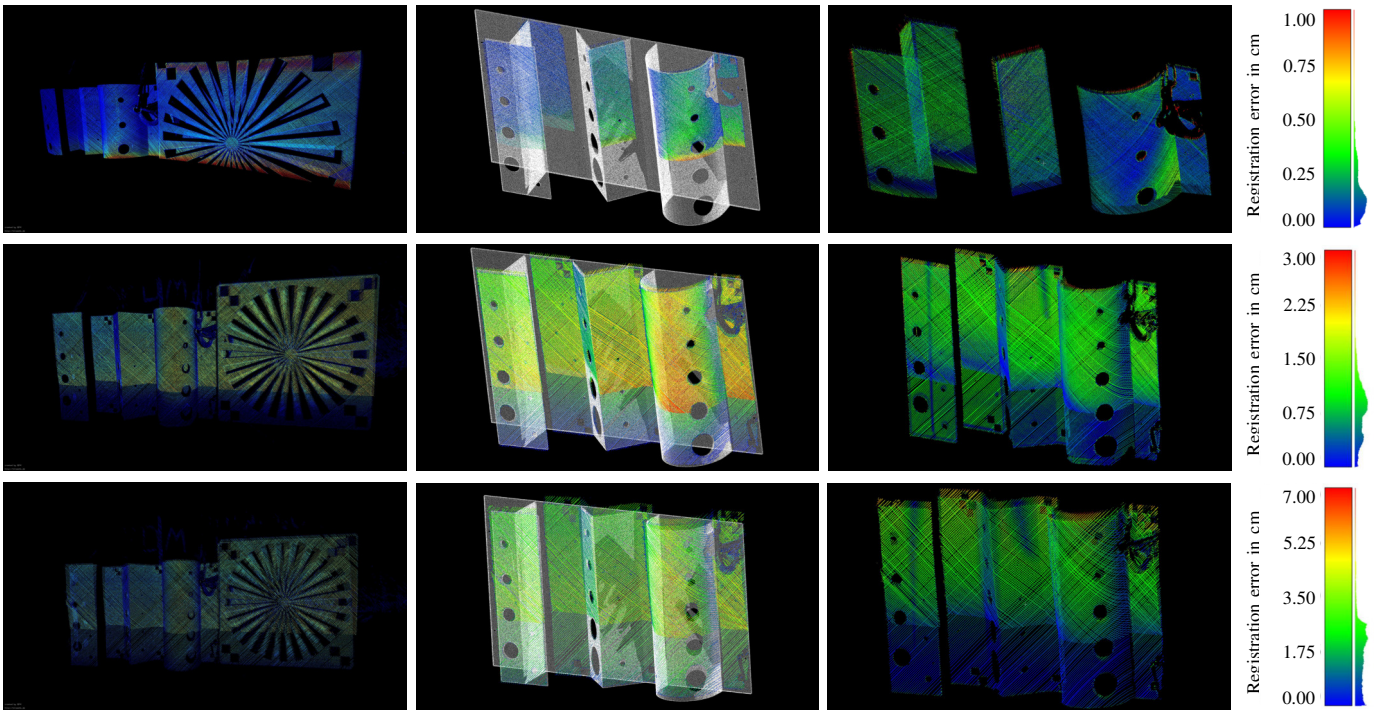

Fig. 8. Scans of the test objects captured at different distances of $1\,\mathrm{m}$, $2\,\mathrm{m}$ and $3.5\,\mathrm{m}$ (from top to bottom). Left: point cloud colored using intensities, middle: registration of the scan with the reference model (white), right: distance between reference model and 3D scan.

misalignment of the measurements of the two laser lines is visible, which is caused by calibration inaccuracies.

B. Underwater Mobile Mapping Results

As a second experiment mobile scans were acquired by moving the scanner in the water using the towing carriage. For this experiment the scanner was moved with constant velocity at a slow speed of $0.1\,\mathrm{m\,s^{-1}}$ through the water. It is assumed that the trajectory is approximately linear. However, the angular parameters of the relative pose of the scanner with respect to the towing carriage need to be estimated from the data.

The result for a trajectory with a length of $8\,\mathrm{m}$ is shown in Figure 9. The red line visualizes the trajectory of the scanner. The top images show two renderings of the point cloud colored by intensities, while the bottom images are colored by height.

For comparison the tank was also scanned from static positions using the scanner's motorized axis. The top images in Figure 10 show $360\,\mathrm{deg}$ scans of the towing tank. The point cloud was created by registering three scans using the ICP algorithm. The individual scanner poses are marked along the red line. The bottom image in Figure 10 shows the difference between the point cloud capture by towing the scanner through the water and the static scans. Both models agree well with the majority of errors below $5\,\mathrm{cm}$. The larger errors in the range of decimeters are a result of no overlap between the two scans due to occlusions, or outliers caused, for example, by reflections on metallic surfaces.

C. Discussion

The first results of the proposed underwater laser scanning system are promising and good quality scans are achieved. The calibration routines need some improvement to increase

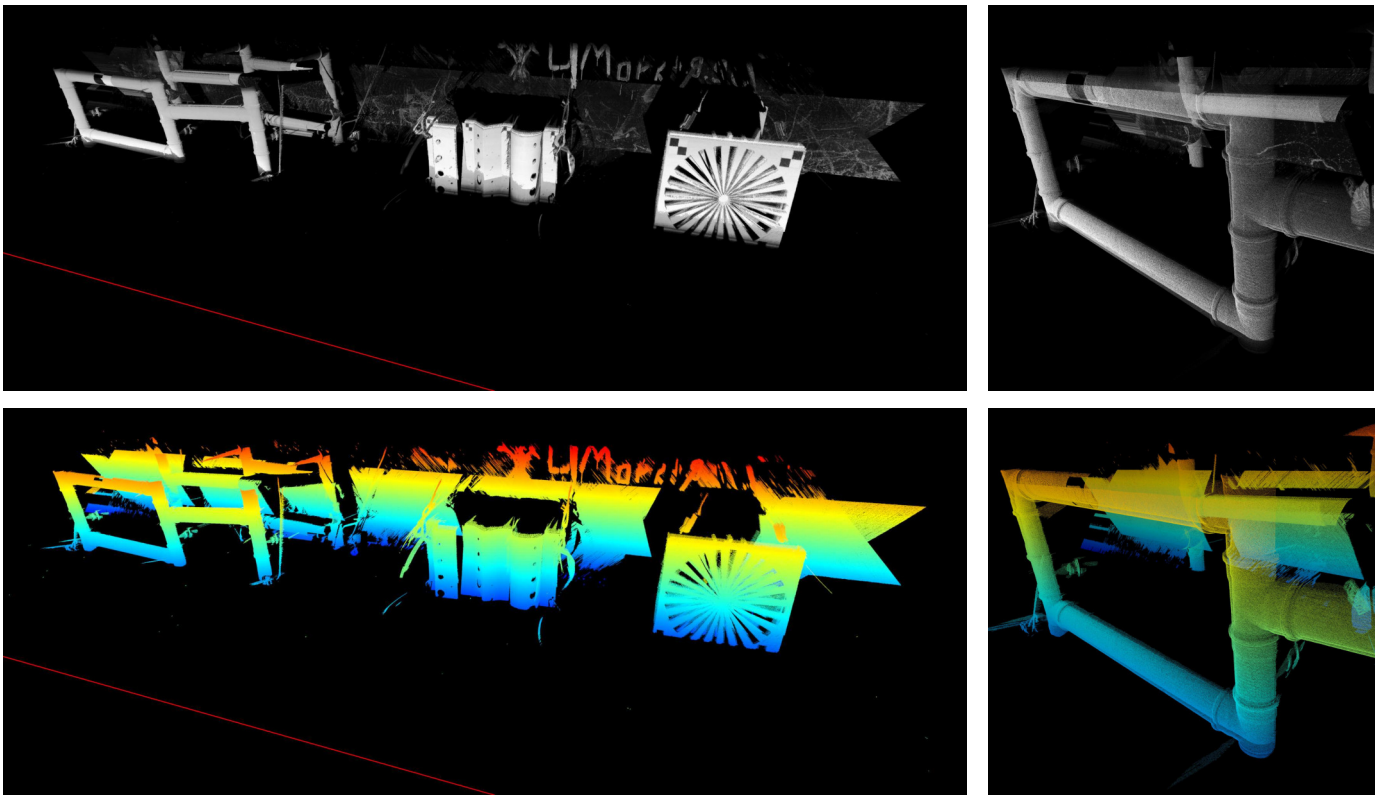

Fig. 9. Underwater scan created by moving the scanner in the water along a linear trajectory (red line). Top: point cloud and detail view colored with intensities, bottom: point clouds colored by height.

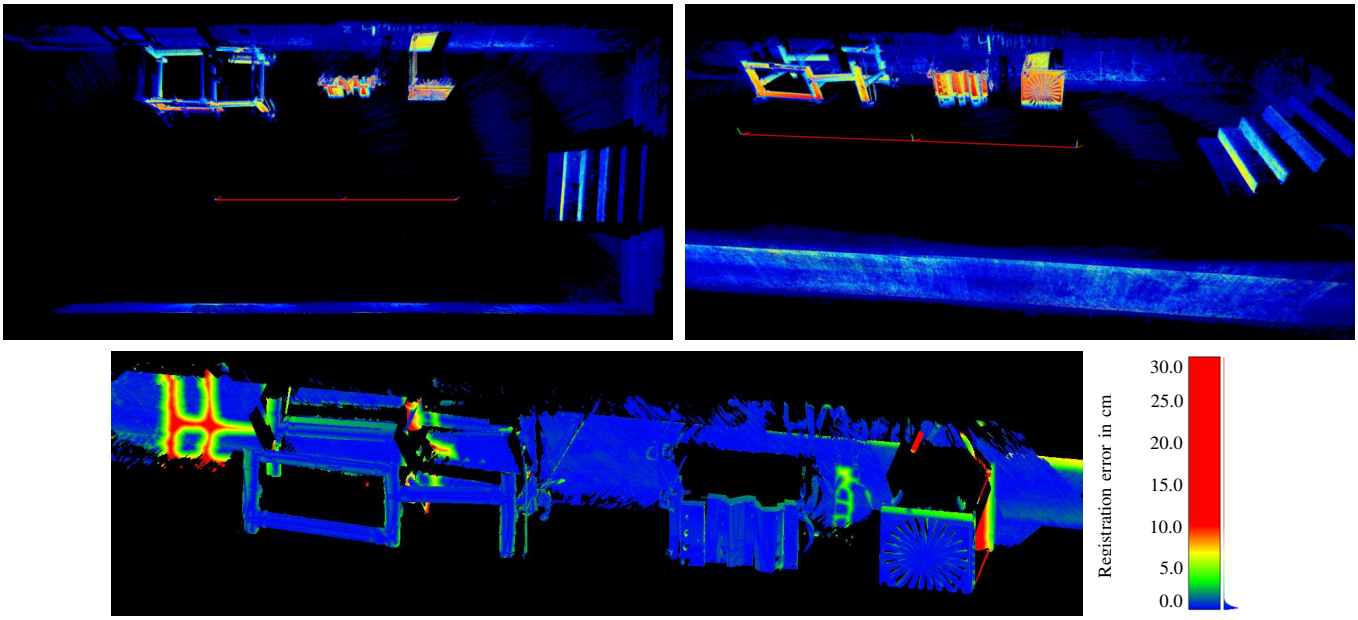

Fig. 10. Comparison between static scans and mobile scans. Top: static scan of the towing tank colored with intensities (the scan poses are marked along the red line), bottom: point distance between the static and mobile mapping scans depicted in Figure 9.

the accuracy of the system. For example, the small L-pattern used in this work for calibration of the laser parameters allows to calibrate only a single line at a time. Using a large calibration fixture and calibrating both laser planes simultaneously enables to exploit additional constraints, such as intersections between the laser lines, in order to improve the relative orientation of the two laser planes. Additionally, the presented data in this paper could not be captured with encoder feedback due to a hardware failure. Therefore, all scans were computed using only the setpoint of the stepper motor, which has a lower angular resolution and is less accurate than the encoder feedback.

V. Conclusions

In this work we presented a structured light underwater laser scanning system and its application for mobile mapping. First experiments and results of acquiring static and mobile scans in a towing tank were described. Using structured light scanners for mobile mapping is interesting because it enables to map larger areas in the water despite the limited measurement range of optical scanners. Needless to say a lot of work remains to be done to apply the proposed scanning system in the field to create precise and repeatable scans in natural waters. In future work we plan to exploit the overlapping scan pattern for simultaneous localization and mapping to improve the trajectory estimates.

Acknowledgment

This work was funded by the project "Mobile Unterwasserkartierung vom Schiff zur hochpräzisen 3D-Erfassung mittels Laserscannen" under the Central Innovation Programme by the German Federal Ministry for Economic Affairs and Energy (ZIM; No. ZF4117504DF8). Part of the work was supported by the European Union's Horizon 2020 research and innovation programme under the grant agreement No 642477.

The authors would like to thank the project "Offshore Wind Solution Mecklenburg Vorpommern (2015 - 2018)" and the partners Fraunhofer IGP in Rostock and IMAWIS GmbH for the support and cooperation during the experiments in the towing tank. Special thanks to Dr.-Ing. Frank Niemeyer from Fraunhofer IGP in Rostock and Matthias Neummann from IMAWIS GmbH for the organization of the trials. Thanks to Rene Diederich from IMAWIS for the support with crane operations and the teams from Leibniz Institute for Baltic Sea Research and Kraken Robotics for the cooperation during the experiments. Many thanks to Dr.-Ing. Andreas Wolter and his team from the chair of fluid mechanics at the University of Rostock for providing and operating the test facilities.

References

[1] F. Menna, P. Agrafiotis, and A. Georgopoulos, "State of the art and applications in archaeological underwater 3D recording and mapping," *Journal of Cultural Heritage*, vol. 33, pp. 231–248, Sep. 2018.

[2] M. Massot-Campos and G. Oliver-Codina, "Optical Sensors and Methods for Underwater 3D Reconstruction," *Sensors*, vol. 15, no. 12, pp. 31 525–31 557, Dec. 2015.

[3] N. Törnblom, "Underwater 3D Surface Scanning Using Structured Light," Master's thesis, Uppsala University, 2010.

[4] C. Bräuer-Burchardt, M. Heinze, I. Schmidt, P. Kühmstedt, and G. Notni, "Underwater 3D Surface Measurement Using Fringe Projection Based Scanning Devices," *Sensors*, vol. 16, no. 1, Jan. 2016.

[5] F. Bruno, G. Bianco, M. Muzzupappa, S. Barone, and A. V. Razionale, "Experimentation of structured light and stereo vision for underwater 3D reconstruction," *ISPRS Journal of Photogrammetry and Remote Sensing*, vol. 66, no. 4, pp. 508–518, Jul. 2011.

[6] 2G Robotics, "ULS-500 underwater laser scanner," http://www.2grobotics.com/products/underwater-laser-scanner-uls-500/, webpage, accessed April 1, 2019.

[7] A. Palomer Vila, P. Ridao Rodríguez, D. Youakim, D. Ribas Romagós, J. Forest Collado, and Y. R. Petillot, "3D Laser Scanner for Underwater Manipulation," *Sensors*, vol. 18, no. 4, Apr. 2018.

[8] A. Palomer, P. Ridao, D. Ribas, and J. Forest, "Underwater 3D Laser Scanners: The Deformation of the Plane," in *Sensing and Control for Autonomous Vehicles*, ser. Lecture Notes in Control and Information Sciences, T. I. Fossen, K. Y. Pettersen, and H. Nijmeijer, Eds. Springer, Cham, May 2017, vol. 474, pp. 73–88.

[9] A. Martins, J. Almeida, C. Almeida, A. Dias, N. Dias, J. Aaltonen, A. Heininen, K. T. Koskinen, C. Rossi, S. Dominguez, C. Vörös, S. Henley, M. McLoughlin, H. van Moerkerk, J. Tweedie, B. Bodo, N. Zajzon, and E. Silva, "UX 1 system design – A robotic system for underwater mining exploration," in *2018 IEEE/RSJ International Conference on Intelligent Robots and Systems (IROS)*, Oct. 2018, pp. 1494–1500.

[10] Kraken Robotics, "Kraken SeaVision subsea 3D laser imaging system," https://krakenrobotics.com/products/seavision/, webpage, accessed April 1, 2019.

[11] H. Morinaga, H. Baba, M. Visentini-Scarzanella, H. Kawasaki, R. Furukawa, and R. Sagawa, "Underwater Active Oneshot Scan with Static Wave Pattern and Bundle Adjustment," in *Image and Video Technology, PSIVT 2015*, ser. Lecture Notes in Computer Science, T. Bräunl, B. McCane, M. Rivera, and X. Yu, Eds. Springer, Cham, Feb. 2016, vol. 9431, pp. 404–418.

[12] M. Massot-Campos and G. Oliver-Codina, "Underwater Laser-based Structured Light System for one-shot 3D reconstruction," in *Proceedings of IEEE Sensors 2014*, Nov. 2014, pp. 1138–1141.

[13] M. Bleier and A. Nüchter, "Low-cost 3D Laser Scanning in Air or Water Using Self-calibrating Structured Light," in *Proceedings of the 7th ISPRS International Workshop 3D-ARCH 2017: "3D Virtual Reconstruction and Visualization of Complex Architectures"*, ser. ISPRS Archives Photogrammetry and Remote Senssing Spatial Inf. Sci., Volume XLII/W3, Nafplio, Greece, March 2017, pp. 105–112.

[14] 3D at Depth, "SL1 subsea lidar," https://www.3datdepth.com/product/sl1-lidar-laser, 2016, webpage, accessed January 20, 2017.

[15] M. Imaki, H. Ochimizu, H. Tsuji, S. Kameyama, T. Saito, S. Ishibashi, and H. Yoshida, "Underwater three-dimensional imaging laser sensor with 120-deg wide-scanning angle using the combination of a dome lens and coaxial optics," *Optical Engineering*, vol. 56, no. 3, Oct. 2017.

[16] ADUS Deepocean, "High-quality surveys of man-made structures as an aid to improved decision making," https://www.video.teledynemarine.com/video/10368962/high-quality-surveys-of-man-made-structures-as-an, webpage, accessed April 1, 2019.

[17] A. Duda, J. Schwendner, and C. Gaudig, "SRSL: Monocular self-referenced line structured light," in *Proceedings of the IEEE/RSJ International Conference on Intelligent Robots and Systems (IROS)*, Sep. 2015, pp. 717–722.

[18] C. Steger, "An unbiased detector of curvilinear structures," *IEEE Transactions on Pattern Analysis and Machine Intelligence*, vol. 20, no. 2, pp. 113–125, Feb. 1998.

[19] Z. Zhang, "A flexible new technique for camera calibration," *IEEE Transactions on Pattern Analysis and Machine Intelligence*, vol. 22, no. 11, pp. 1330–1334, Nov. 2000.

[20] E. Olson, "AprilTag: A robust and flexible visual fiducial system," in *Proceedings of the 2011 IEEE International Conference on Robotics and Automation (ICRA)*, May 2011, pp. 3400–3407.

[21] Nikon Metrology, "iSpace / iGPS - Factory-wide measuring, positioning and tracking system," https://www.nikonmetrology.com/es/product/igps, webpage, accessed April 1, 2019.

[22] F. Niemeyer, M. Neumann, J. Albiez, A. Duda, and M. Geist, "Untersuchungen zur Messgenauigkeit von Laserscannern unter Wasser am Beispiel des SeaVision 3D Laser System," in *Photogrammetrie Laserscanning Optische 3D-Messtechnik, Beiträge der Oldenburger 3D-Tage 2018, Jade Hochschule*, Feb. 2018, to appear.